Reactions of manganese iminoacyl complexes with phosphines, phosphites and sulfur dioxide

Christine L. Braun*, John J. Alexander** and Douglas M. Ho†

Department of Chemistry, University of Cincinnati, Cincinnati, OH 45221-0172 (USA)

(Received November 25, 1991; revised March 24, 1992)

Abstract

Reactions involving the Mn–N bond of tetracarbonyl[1,2-bis(*p*-tolylimino)-3-(*p*-chlorophenyl)propyl]manganese, and some of its tricarbonyl derivatives containing phosphine or phosphite ligands were investigated. In an effort to prepare complexes with non-chelated bis(iminoacyl) ligands, this Mn compound was allowed to react with phosphines and phosphites. Only products of carbonyl substitution were obtained. All these compounds were allowed to react with sulfur dioxide. The SO_2 adducts were unstable and had CO stretching frequencies 20–30 cm^{-1} higher than those of the parent phosphine or phosphite compounds. Evidence is presented for nucleophilic attack by SO_2. The molecular structure of $Mn(CO)_3[P(OCH_2)_3CCH_2CH_3][C(=N\text{-}C_6H_4CH_3)C(=NC_6H_4\text{-}CH_3)CH_2C_6H_4Cl]$ has been determined by X-ray diffraction. Also investigated were reactions of tetracarbonyl [1,2-bis(*p*-tolyl-imino)-3-*p*-chlorophenyl)propyl] manganese with SO_3, tetracyanoethylene and 1,1-diphenylethylene. Instead of the anticipated imino N displacement and ring closure, SO_3 gave only oxidation products while the olefins did not react.

Introduction

Tetracarbonyl[1,2-bis(*p*-tolylimino)-3-(*p*-chlorophenyl)propyl]manganese (**I**) is known to undergo insertion reactions into the Mn–N bond [1]. Motz *et al.* allowed I to react with one equivalent cyclohexyl isocyanide in toluene, at ambient temperature for 24 h and obtained **II** and **III**.

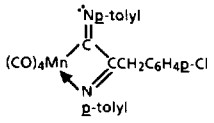

I

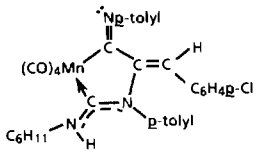

II

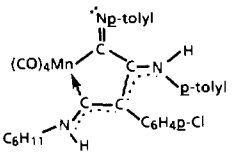

III

In contrast **I** reacted with one equivalent of t-butylisocyanide to give **IV** and **V**.

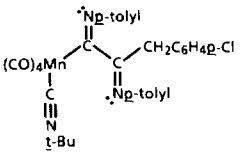

IV (40%)

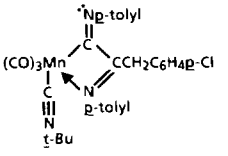

V (27%)

If **IV** is not kept under CO, the iminoacyl N lone pair displaces a carbonyl converting it to **V**. These results suggest that the formation of **II** and **III** results from displacement of the coordinated N lone pair in **I** by isocyanide and subsequent ring closure by reattack on the polarized isocyanide ligand. The bulky t-butyl group prevents this attack leading to **IV** and **V** instead.

Bouligarakis [2] refluxed **I** in neat sulfur dioxide giving an almost insoluble red complex which contained SO_2. It seemed likely that biphilic SO_2 behaves similarly to isocyanide, initially displacing coordinated N from Mn by nucleophilic attack and then possibly suffering attack by N at the electrophilic center to form a ring. Unfortunately, the insolubility of this compound has prevented its complete characterization.

Therefore it was of interest to see whether stable compounds such as **IV** with a 'dangling' iminoacyl group could be prepared and also whether other biphilic reagents, such as olefins, or sulfur trioxide, could be inserted into the manganese–nitrogen bond. Another goal was to investigate the effects of changes in electron

*Present address: University of Stuttgart, FRG.

**Author to whom correspondence should be addressed.

†Present address: Department of Chemistry, Princeton University, USA.

0020-1693/92/$5.00

density or steric hindrance at the metal on reactions at the Mn–N bond.

Experimental

All IR spectra were recorded in dichloromethane or chloroform with a Perkin-Elmer 1600 FT-IR spectrophotometer, using sodium chloride (0.5 cm) cells. For spectral intensities the abbreviations w, m, s, br and sh refer to weak, medium, strong, broad and shoulder, respectively. Proton nuclear magnetic resonance spectra were obtained on an IBM NR-80 instrument in Fourier transform mode. Positive chemical shifts are given in ppm downfield from tetramethylsilane as an internal standard. Spectral values are reported as follows: s = singlet, d = doublet, t = triplet, q = quartet, m = multiplet.

Analytical thin-layer chromatography was conducted using E. Merck silica gel 60-PF 254 precoated plates. Compounds were made visible by UV light (254 nm). Preparative chromatographic separations were obtained by column chromatography using neutral alumina 80–200 mesh or silica gel finer than 220 mesh.

Melting points were determined on a Mel-Temp apparatus using closed capillaries and are uncorrected.

Low-resolution mass spectra were obtained on a Hewlett-Packard 5995 A quadrupolar GC/MS system by means of direct inlet. High-resolution mass spectra were obtained on a Kratos MS801-DS55 spectrometer.

Elemental analysis was performed by Galbraith Laboratories, Inc., Knoxville, TN.

Dimanganese decacarbonyl was purchased from the Pressure Chemical Company and used as received; anhydrous grade sulfur dioxide was purchased from Matheson. All other laboratory chemicals were reagent grade and were used as received.

Tetrahydrofuran (thf) was distilled from calcium hydride immediately before use; toluene was dried with calcium chloride and distilled. Acetone, acetonitrile and carbon tetrachloride were purified by standard literature methods [3]. Diethyl ether was anhydrous grade (Fisher) and used as received. All other solvents were reagent grade and freshly distilled before use.

N-p-Tolylformamide [4, 5] and *p*-tolyl isocyanide [6] were prepared and purified by methods reported in the literature. [(*p*-Chloro)benzyl]pentacarbonylmanganese and tetracarbonyl[2,3-bis(*p*-tolylimino)-3-(*p*-chlorophenyl)propyl]manganese (**I**) were prepared using the procedures reported in ref. 1.

Preparation of tricarbonyl(phosphine)[1,2-bis(p-tolylimino)-3-(p-chlorophenyl)propyl]manganese (VI, VII) and tricarbonyl(phosphite)[1,2-bis(p-tolylimino)-3-(p-chlorophenyl)propyl]manganese (VIII–X)

General procedure

The bis(imino) complex **I** (260 mg, 0.50 mmol) and phosphine or phosphite (0.50 mmol) were dissolved in 10 ml thf and refluxed under nitrogen for 7 h. Solvent was removed *in vacuo*, the residue taken up with a minimum amount of chloroform and chromatographed using a column packed with SiO_2 in hexanes. For separation on the column gradient elution with 100:0 to 50:50 vol.:vol. hexane:dichloromethane solutions was employed. Normally no unreacted **I** was found. If any was present, it was eluted before the substituted compounds. All the phosphine and phosphite compounds are soluble in CH_2Cl_2 or $CHCl_3$ and insoluble in hexanes.

$Mn(CO)_3(PCy_3)[C(=NC_6H_4P\text{-}CH_3)C(=N\text{-}C_6H_4P\text{-}CH_3)CH_2C_6H_4P\text{-}Cl]$ (VI)

The sole product was **VI** obtained as a brick red powder. Yield 330 mg (0.43 mmol, 85%). Melting point 142–143 °C. Spectral data: ^{1}H NMR ($CDCl_3$): 7.30–6.85 (m, 12H); 3.87 (dd, 2H, J = 13.1 Hz); 2.36 (s, 3H), 2.38 (s, 3H); 2.1–0.8 (m, 33H). IR (CH_2Cl_2): CO 1994 (s), 1912 (s), 1889(s); C=N 1604 (m). *Anal.* Calc. for $C_{44}H_{53}ClMnN_2O_3P$: C, 67.81; H, 6.85; N, 3.60. Found: C, 68.33; H, 7.01; N, 3.57%.

$Mn(CO)_3(PPh_3)[C(=NC_6H_4P\text{-}CH_3)C(=N\text{-}C_6H_4P\text{-}CH_3)CH_2C_6H_4P\text{-}Cl]$ (VII)

Brick red **VII** was the sole product. Yield 304 mg (0.40 mmol, 80%). Melting point 148–149 °C. Spectral data: ^{1}H NMR ($CDCl_3$): 7.25–6.74 (m, 27H), 3.43 (dd, 2H, J = 13.6 Hz) 2.39 (s, 3H), 2.33 (s, 3H). IR ($CHCl_3$): CO 2004 (s), 1927 (s), 1902 (s); C=N 1609 (m). *Anal.** Calc. for $C_{44}H_{35}ClMnN_2O_3P$: C, 60.43; H, 4.64; N, 3.68. Found: C, 69.48; H, 4.51; N, 3.51%.

$Mn(CO)_3[P(OCH_3)_3][C(=NC_6H_4P\text{-}CH_3)C(=N\text{-}C_6H_4P\text{-}CH_3)CH_2C_6H_4P\text{-}Cl]$ (VIII)

The final chromatographic eluent contained 66% methylene chloride. Besides one red compound, **VIII**, there were some unidentified yellow and green by-products. Yield 248 mg (0.40 mmol, 80%). Melting point 97–98 °C. Spectra data: ^{1}H NMR ($CDCl_3$): 7.20–6.80 (m, 12H), 3.93 (dd, 2H, J = 10.8Hz), 3.33 (d, 9H, J = 10.9), 2.34 (s, 3H), 2.32 (s, 3H). IR (CH_2Cl_2): CO 2013 (s), 1940 (s), 1908 (s); CN 1616 (m). *Anal.* Calc. for $C_{29}H_{29}ClMnN_2O_6P$: C, 55.91; H, 4.69; N, 4.50. Found: C, 55.79; H, 4.97; N, 3.96%.

*Sample prepared by P. Motz (see ref. 9).

$Mn(CO)_3[P(OPh)_3][C(=NC_6H_4P\text{-}CH_3)C(=N\text{-}C_6H_4P\text{-}CH_3)CH_2C_6H_4P\text{-}Cl]$ (IX)

Separation on a column gave two different carbonyl-containing products and, as in reaction with $P(OMe)_3$, some unidentified green and yellow byproducts. The first product was a purple oil (1.09 mg) and was not investigated, the second one a red solid, **IX**. Yield 316 mg (0.39 mmol, 78%). Melting point 117–118 °C. Spectral data: ^{1}H NMR ($CDCl_3$) 7.32–6.75 (m, 27H), 3.85 (s, 2H), 2.46 (s, 3H), 2.44 (s, 3H). IR (CH_2Cl_2): CO 2019 (s), 1950 (s), 1918 (s); C=N 1616 (m). *Anal.* Calc. for $C_{44}H_{35}ClMnN_2O_6P$: C, 65.30; H, 4.36; N, 3.46. Found: C, 64.47; H, 4.45; N, 2.59%.

$Mn(CO)_3[P(OCH_2)_3CCH_2CH_3][C(=NC_6H_4P\text{-}CH_3)C(=NC_6H_4P\text{-}CH_3)CH_2C_6H_4P\text{-}Cl]$ (X)

This compound decomposed at the reflux temperature of thf; therefore another method was used. Bis(imino) complex **I** (260 mg, 0.50 mmol), $P(OCH_2)_3CC_2H_5$ (81 mg, 0.50 mmol) and trimethylamine-*N*-oxide dihydrate (56 mg, 0.50 mmol) were dissolved in 10 ml methylene chloride and stirred under nitrogen at room temperature for 24 h. The solution was reduced in volume and chromatographed on a SiO_2 column. As with **VIII**, the final eluent contained 66% methylene chloride. One orange product, **X**, was obtained. Yield 328 mg (0.48 mmol, 95%). Melting point 170 °C, dec. Spectral data: ^{1}H NMR ($CDCl_3$): 7.27–6.80 (m, 12H), 4.07 (d, 6H, J=4.1), 3.73 (dd, 2H, J=13.1), 2.38 (s, 3H), 2.36 (s, 3H), 1.18 (q, 2H), 0.81 (t, 3H). IR (CH_2Cl_2): CO 2021 (s), 1950 (s), 1919 (s); C=N 1619 (m). *Anal.* Calc. for $C_{32}H_{31}ClMnN_2O_6P$: C, 58.15; H, 4.73; N, 4.24. Found: C, 58.08; H, 5.01; N, 3.51%.

Reaction of sulfur dioxide with the phosphine or phosphite compounds, VI–X

General procedure [7]

About 100 mg of phosphine or phosphite compound and a stirring bar were introduced into a 25 ml flask fitted with a vacuum adapter connected with the SO_2 tank and a dry ice condenser. The condenser was attached to a mineral oil bubbler while the apparatus was flushed with dried nitrogen and after that with anhydrous sulfur dioxide. The connection to the bubbler and the SO_2 tank was closed, the condenser filled with dry ice and the apparatus set on dry ice for the time needed to condense 10 ml of sulfur dioxide into the flask. The resulting solution was allowed to reflux for 15 h, cooled to −70 °C overnight, then refluxed for an additional 11 h. Excess SO_2 was evaporated and the apparatus opened under positive N_2 pressure. The resulting mixtures of SO_2 complex, starting material and decomposition products could not be separated, because the SO_2 complexes were unstable in organic solvents and sensitive to humidity. They decomposed totally on SiO_2 columns and partially when SO_2 was removed at reduced pressure or when they were heated. Therefore, no analytical data could be obtained. All spectra were taken with the crude product mixtures.

The solubilities of SO_2 adducts and starting complexes in thf, CH_2Cl_2 and $CHCl_3$ were similar. Hence, bubbling SO_2 through solutions of **VI–X** did not precipitate **XI–XV**.

$Mn(CO)_3(PCy_3)(SO_2)[C=N(C_6H_4P\text{-}CH_3)C(=N\text{-}(C_6H_4P\text{-}CH_3)CH_2C_6H_5P\text{-}Cl]$ (XI)

Color: brick red. Yield 41%. ^{1}H NMR ($CDCl_3$): 7.30–6.80 (m, 12H), ~4.1 (s, 2H), 2.38 (s, 3H), 2.36 (s, 3H), 2.1–0.8 (m, 33H). IR (CH_2Cl_2): CO 2017 (s), 1949 (s), 1926 (s); C=N 1613 (m); SO 1263 (w), 1048 (w).

$Mn(CO)_3(PPh_3)(SO_2)[C=N(C_6H_4P\text{-}CH_3)C(=N\text{-}(C_6H_4P\text{-}CH_3)CH_2C_6H_5P\text{-}Cl]$ (XII)

Color: brick red. Yield 48%. ^{1}H NMR ($CDCl_3$): 7.53–6.33 (m, 27H), 3.77 (dd, 2H, J=14.9), 2.35 (s, 3H), 2.33 (s, 3H). IR (CH_2Cl_2): CO 2026 (s), 1963 (s), 1935 (s); C=N 1616 (m); SO 1263 (w), 1040 (w).

$Mn(CO)_3[P(OMe)_3](SO_2)[C=N(C_6H_4P\text{-}CH_3)C(=N(C_6H_4P\text{-}CH_3)CH_2C_6H_5P\text{-}Cl]$ (XIII)

Color: red. Yield 74%. ^{1}H NMR ($CDCl_3$): 7.30–6.80 (m, 12H), ~4.6 (dd, 2H), 3.75 (d, 9H, J=10.8), 2.40 (s, 3H), 2.38 (s, 3H). IR (CH_2Cl_2): CO 2042 (s), 1962 (s), 1940 (s); C=N 1611 (m); SO 1241 (m), 1038 (m).

$Mn(CO)_3[P(OPh)_3](SO_2)[C=N(C_6H_4P\text{-}CH_3)C(=N\text{-}(C_6H_4P\text{-}CH_3)CH_2C_6H_5P\text{-}Cl]$ (XIV)

Color: red. Yield 62%. ^{1}H NMR ($CDCl_3$): 7.33–6.64 (m, 27H), ~4.03 (dd, 2H), ~2.4 (s, 3H), ~2.4 (s, 3H). IR (CH_2Cl_2): CO 2045 (s), 1958 (s,br); C=N 1611 (m); SO 1250 (m), 1038 (w).

$Mn(CO)_3[P(OCH_2)_3CCH_2CH_3](SO_2)[C=N(C_6H_4P\text{-}CH_3)C(=N(C_6H_4P\text{-}CH_3)CH_2C_6H_5P\text{-}Cl]$ (XV)

Color: orange. Yield 100%. ^{1}H NMR ($CDCl_3$): 7.80–7.27 (m, 12H), 4.22 (dd, 2H), 4.22 (d, 6H, J=6.0), 2.40, 2.36 (s, 3H), 1.34 (t, 3H), 0.93 (q, 2H). IR (CH_2Cl_2): CO 2049 (s), 1975 (s), 1953 (s); C=N 1612 (m); SO 1240 (m), 1030 (m).

X-ray diffraction of X

To grow crystals suitable for X-ray diffraction, **X** was dissolved in a minimum amount of methylene chloride, the solution was filtered and crystals grown by means of vapor diffusion using pentane as the second solvent. The sample consisted of air-stable orange plates and prisms. A suitably large crystal was isolated, cut to roughly 0.15×0.22×0.42 mm in size, mounted on a

glass fiber with epoxy cement, and transferred to a Nicolet R3m four-circle diffractometer for characterization and data collection.

The unit cell parameters were subsequently determined from the angular settings of 25 well-centered reflections (within the range $20 < 2\theta < 32°$) and were as follows: $a = 10.438(2)$, $b = 18.449(3)$, $c = 16.278(2)$ Å, $\beta = 92.21°$ and $V = 3132.2(8)$ Å^3. Axial photographs and a limited search through an octant of reciprocal space revealed systematic absences and symmetry consistent with the monoclinic space group $P2_1/c$.

One quadrant of data ($\pm h$, $+k$, $+l$) was collected in the 2θ–θ scan mode with 2θ ranging from 3.0 to 55.0°. Scan speeds were varied from 4.0 to 8.0°/min. A total of 7719 reflections was measured and corrected for Lorentz and polarization effects, but not for absorption. The minimun and maximum drift corrections (based on a set of 3 standards measured for every 37 reflections) were 0.9827 and 1.0034, respectively. Data processing yielded 7237 unique reflections of which 2863 had $F > 6\sigma(F)$ with $R(\text{int}) = 0.0231$ for the averaging of equivalent reflections.

The structure was successfully solved by heavy-atom methods (XS:PATT) in the monoclinic space group $P2_1/c$ (No. 14), and refined by full-matrix least-squares. Table 1 gives parameters connected with the X-ray structure determination.

Results and discussion

In an effort to prepare $Mn(CO)_4(PR_3)[C(=NC_6H_4P\text{-}CH_3)C(=NC_6H_4P\text{-}CH_3)\text{-}CH_2C_6H_4P\text{-}Cl]$ with 'dangling' rather than chelating bis(iminoacyl) ligands, we attemptcd to displace the coordinated iminoacyl N in **I** by phosphines or phosphites without loss of CO. The bis(imino) complex **I** and one equivalent phosphine or phosphite were stirred in thf under nitrogen at room temperature. The rate of the reaction was very low. After one week of stirring large amounts of **I** remained. For example, only 30% of a sample of **I** reacted with PPh_3 over one week at room temperature. Separation by chromatography afforded only unreacted starting material and small amounts of the CO-substituted complexes **VI–X**.

It seems likely that phopshines and phosphites are sufficiently nucleophilic to attack Mn displacing the imino N. However, as in the reaction of **I** with t-BuNC, the imino N goes on to displace CO leading to the tricarbonyl products as indicated in Scheme 1.

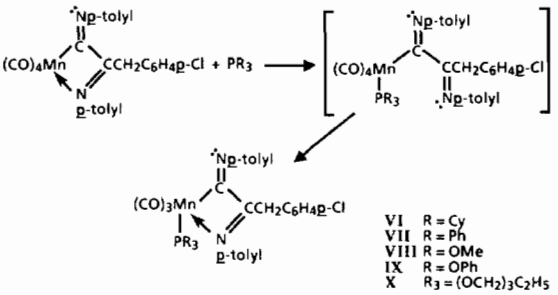

Scheme 1.

In order to prepare sufficient quantities of **VI–X** for characterization, the reactions were conducted at reflux. In the case of the $P(OCH_2)_3CC_2H_5$ compound, CO could be substituted using this method, but the elevated temperature afforded too many byproducts for convenient purification, so that another method was used. Treatment of the bis(imino) complex **I** with $P(OCH_2)_3CC_2H_5$ and trimethylamine-*N*-oxide dihydrate in methylene chloride at ambient temperature led to the formation of **X** as the only product in very high yield. Trimethylamine-*N*-oxide has been shown to promote the stoichiometric loss of coordinated CO from transition metal complexes [8]. **VII** has previously been prepared in this way [9]. The reason for the formation of so many byproducts with $P(OCH_2)_3CC_2H_5$ is unclear. The mechanism of uncatalyzed ligand displacement in **I** has not yet been studied. However, the fact that PCy_3 having a cone angle of 170° [10] reacts easily is some evidence in favor of the problem with $P(OCH_2)_3CC_2H_5$ (cone angle 101°) being other than steric. Insofar as pK_a can be used as a measure of nucleophilicity, $P(OPh)_3$ (pK_a −2.0 [11]) should be less nucleophilic than $P(OCH_2)_3CC_2H_5$ (pK_a 1.74 [11]). Yet $P(OPh)_3$ reacts without difficulty. Moreover, the cage phosphite should certainly be stable in dry, refluxing thf.

Since $AsPh_3$ is known to be less nucleophilic than phosphines or phosphites [12], its ability to displace imino N was in doubt. Thus, in the attempted reaction of **I** with $AsPh_3$, PdO was used as a catalyst to effect direct CO displacement [13]. The fact that only decomposition was observed is consistent with $AsPh_3$ being too weak a nucleophilic to attack at an appreciable rate the species produced by reaction of **I** with PdO.

Attempted reaction of **I** with olefins, tetracyanoethylene and 1,1-diphenylethylene led to a mixture of uncharacterizable products and to no reaction respectively. SO_3 gave only oxidation products.

Spectral properties of **VI–X** are in agreement with the *fac* structure. In the IR spectra all these compounds show three sharp bands of nearly equal intensity in the range 1899–2021 cm^{-1}. This is consistent with a $(CO)_3ML_3$ complex with the COs arranged in a *facial* geometry [14]. Two bands very close together centered around 1610 cm^{-1} are assigned to the C=N stretching

TABLE 1. Structure determination summary for $C_{32}H_{31}ClMnN_2O_6P$

Crystal data	
Formula	$C_{32}H_{31}ClMnN_2O_6P$
Color and habit	orange plates and prisms
Size (mm)	0.15×0.22×0.42
Crystal system	monoclinic
Space group	$P2_1/c$ (No. 14)
Unit cell dimensions	
a (Å)	10.438(2)
b (Å)	18.449(3)
c (Å)	16.278(2)
β (°)	92.21(1)
Volume (Å^3)	3132.2(8)
Z (formulae/cell)	4
Formula weight	660.97
Density, calc. (g/cc)	1.40
Absorption coefficient (cm^{-1})	5.84
$F(000)$ (e^-)	1368
Data collection	
Diffractometer	Nicolet R3m
Radiation	Mo Kα (λ=0.71073 Å)
Monochromator	highly oriented graphite crystal
Temperature (K)	294
2θ Range (°)	3.0–55.0
h, k, l Limits	−14→14, 0→24, 0→22
Scan type	2θ–θ
Scan speed (°/min)	variable; 4.0 to 8.0
Scan range (°)	0.75 on either side of Kα 12
Background measurement	stationary crystal and counter at beginning and end of scan; total background time to scan time ratio of 0.5
Standard reflections	3 measured every 37
Reflections collected	7719 total; 7237 independent; R(int)=0.0231
Reflections observed	2863; $F>6*\sigma(F)$
Absorption correction	N/A
Min./max. transmission	N/A
Solution and refinement	
System used	Nicolet SHELXTL PLUS (Micro VAX II)
Solution	sharpened Patterson (XS:PATT)
Refinement method	full-matrix least-squares (XLS)
Absolute configuration	N/A
Extinction correction	N/A
Final residuals	$R(F)$=0.0495 R_w(F)=0.0460
Goodness-of-fit	S=1.43
Max. and mean (shift/e.s.d.)	0.001 and 0.000
No. variables	388
Data-to-parameter ratio	7.4:1
Max./min. excursions (e$^-$/A^3)	0.29 and −0.28

of the two imino double bonds. In the ^{1}H NMR spectra of all but one (the $P(OPh)_3$ complex **IX**), the two benzylic protons appear as AB quartet centered at 3.87 (PCy_3), 3.43 (PPh_3), 3.93 ($P(OMe)_3$) and 4.07 ($P(OCH_2)_3CC_2H_5$). **I** also shows this AB quartet that can be attributed to the lack of a plane of symmetry which makes the two protons magnetically inequivalent. The chemical shift of these two protons is rather sensitive to changes in the P-containing ligand. Surprisingly, the $P(OPh)_3$ complex shows only a singlet at 3.85. Even at 250 MHz no resolution of the singlet is achieved. We can only suggest that an accidental degeneracy in chemical shift of the benzylic protons leads to the appearance of the singlet in the $P(OPh)_3$ complex. The other peaks of the spectra can be straightforwardly assigned to the other protons of the molecule. Low-resolution mass spectra of all of these compounds were taken, but (except with **VIII**) the only fragments found were $Mn(CO)_3^+$, $Mn(CO)_2^+$, $Mn(CO)^+$, $(C_8H_7N)^+$, $(MnC_2N)^+$, $(C_9H_6N)^+$, $(C_7H_7N)^+$, $(C_7H_7)^+$ and fragments of the phosphines or phosphites. So, these results are not structurally diagnostic. Only in the $P(OMe)_3$ compound **VIII** did the low-resolution mass spectrum give the parent peak (calc.: 622.94, found: 622). The

high resolution mass spectrum of **VIII** gave the parent peak at 623.1.

Reaction of SO_2 with VI–X

Refluxing **VI–X** in liquid SO_2 (−10 °C) leads to new products **XI–XV**. The reaction rates at this temperature are very slow and only one of the reactions reached completion. Moreover, the SO_2-containing products are unstable in organic solvents over the time period required for chromatography and are decomposed by chromatography on SiO_2 and by moisture. The phosphine-containing SO_2 adducts **XI** and **XII** decomposed to starting materials and the phosphite-containing adducts **XIII–XV** to unidentified products. Spectral measurements were thus made on freshly synthesized mixtures of the SO_2 adducts with starting compounds except in the case of the $P(OCH_2)_3CCH_2CH_3$ complex **XV** where the reaction reached completion.

Solution IR spectra (in CH_2Cl_2 or $CHCl_3$) of the SO_2 adducts **XI–XV** exhibit three strong CO bands, compatible with a *facial* geometry. These bands are shifted to higher frequencies (1926–2049 cm^{-1}) than those of the starting complexes (1899–2021 cm^{-1}). Although SO_2 is a worse π-acid than CO [15], the magnitude and direction of the shifts are compatible either with attachment of SO_2 directly to the metal [16] replacing the imino N (as in structures **XVI** and **XVII**) or to a ligand (**XVIII**).

Examples are known of carbonyls which contain SO_2 bonded to a ligand instead of the metal. SO_2 is known [17] to behave as a Lewis acid forming adducts with amines. In the present case, it is possible that SO_2 adds at the lone pair of the uncoordinated imino N (structure **XVIII**). Addition of a proton to the imino N in $CpFe(CO)_2C(=NC_6H_{11})CH_2C_6H_4P$-Cl shifts the CO stretching frequencies from 1946 and 2000 cm^{-1} [18] to 1959 and 2042 cm^{-1} [19]. The facile loss of SO_2 from **XI–XV** is difficult to reconcile with structure **XVII** and is not compatible with **XVI** [20, 21].

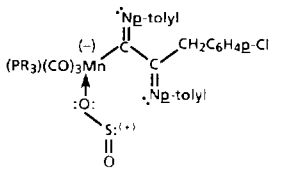

XVI

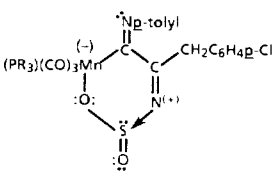

XVII

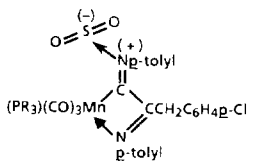

XVIII

Reaction with SO_2 also changes the P–O and C–O vibrations of the phosphite ligands. The frequencies of these vibrations are found in regions where S–O vibrations also occur. The peaks finally assigned as SO vibrations are: (as, s, PR_3): (1263, 1048 cm^{-1}, PCy_3), (1263, 1040 cm^{-1}, PPh_3), (1241, 1038 cm^{-1}, $P(OMe)_3$), (1250, 1038 cm^{-1}, $P(OPh)_3$) and (1240, 1030 cm^{-1}, $P(OCH_2)_3CC_2H_5$). The positions of the asymmetric S–O stretch are outside the ranges quoted [20–22] for structures containing 'sulfone'-type $-\overset{\overset{O}{\|}}{\underset{\underset{O}{\|}}{S}}-$ groups. The large spread in S–O stretching frequencies is reminiscent [20, 21] of the behavior of η^2-O-bonded sulfur dioxide which most often occurs in main-group compounds. However, a transition metal complex containing O-bonded SO_2 $[Mn(OPPh_3)_4(SO_2)_2]I_2$ has been characterized [23] and found to lose one SO_2 reversibly. The low energy S–O stretch is higher by 30 cm^{-1} than typical values for η^2-SO_2 [21]. Also O-bonded SO_2 is difficult to reconcile with shifts in CO stretching frequencies.

Only in the NMR spectrum of **XII** was there a good resolution of the benzylic proton resonances which appear as a doublet of doublets indicating the lack of a plane of symmetry. The positions of the other (less well resolved) benzylic protons indicate shifts of about 0.4 ppm downfield compared to those in **VI–X**.

Available data do not lead to an obvious choice among **XVI**, **XVII** and **XVIII**. However, on the basis of considerations advanced in the next section, and because fragments isoelectronic with d^6 $M(CO)_4$ are expected [21] to form η^1 complexes with SO_2, we favor structure **XVI** or **XVII**.

Mechanistic considerations in reactions of VI–X with SO_2

In order to probe the effects of electronic structure on reactivity of **VI–X** with SO_2, we allowed each complex to reflux in SO_2 for 26 h and immediately measured the IR spectra of the reaction mixtures in CH_2Cl_2. Under these conditions the reaction of **X** went substantially to completion. The relative reactivities of **VI–IX** were estimated by comparing the intensities of the totally symmetric CO stretch for the starting material and for the SO_2 adduct to obtain a relative 'yield' of the product. Of course, such a comparison is only valid on the assumption that the total integrated intensity of each band in the SO_2 adduct is the same as for the parent phosphine or phosphite. The crude numbers obtained are set out in Table 2 along with some pertinent ligand parameters. These numbers are intended to signify only a crude ordering of the reactivities of **VI–X**.

The reactivity of $Mn(CO)_3(PR_3)[C(=N\text{-}C_6H_4P\text{-}CH_3)C(=NC_6H_4P\text{-}CH_3)CH_2C_6H_4P\text{-}Cl]$ with SO_2 de-

TABLE 2. Some properties of $\overline{Mn(CO)_3L[C(=NC_6H_4P\text{-}CH_3)C(=NC_6H_4P\text{-}CH_3)CH_2C_6H_4P\text{-}Cl]}$

L	PCy_3	PPh_3	$P(OMe)_3$	$P(OPh)_3$	$P(OCH_2)_3CH_2CH_3$	CO
Highest energy ν(CO) (cm^{-1})	1994	2004	2013	2019	2021	2073
Cone angle (°)	170	145	107	128	101	
'Yield' of SO_2 adduct	40	48	74	62	100	100

creases in the order $P(OCH_2)_3CC_2H_5 > P(OMe)_3 \approx P(OPh)_3 > PPh_3 \approx PCy_3$. This order seems to rule out electrophilic attack by SO_2 since the values of ν(CO) for **VI–X** reflect an electron density on Mn which decreases in the order $PCy_3 > PPh_3 > P(OMe)_3 > P(OPh)_3 > P(OCH_2)_3CC_2H_5) > CO$. In contrast, $CpFe(CO)(PPh_3)CH_2C_6H_5$ was found [22] to react very rapidly with SO_2 in $CHCl_3$ whereas $CpFe(CO)_2CH_2C_6H_5$ was inert. This points to the behavior of SO_2 as a nucleophile in these reactions and provides evidence against direct electrophilic attack on imino N by SO_2. It is, of course, possible that initial attack at the metal is followed by rearrangement to **XVIII**. The canonical forms **XIXa,b** indicate that attack could occur through either the lone pair on O or on S. We have no evidence bearing on this point.

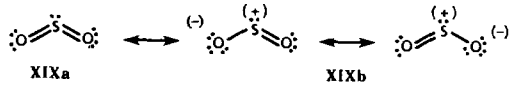

XIXa XIXb

Nucleophilic attack could occur with either dissociative (d) or associative (a) activation. Since, in this case, neither the entering molecule (SO_2) nor the leaving group (presumably imino N) can be varied, we point to the influence of the ancillary ligands PR_3 on the reactivity. d activation should be favored by a large cone angle for PR_3 to promote bond breaking and good Lewis basicity of PR_3 to stabilize an electron-deficient transition state or intermediate. Lewis basicity of PR_3 decreases in the order of electron density on Mn quoted above whereas steric requirements of PR_3 decrease with cone angle in the order $PCy_3 > PPh_3 > P(OPh)_3 > P(OMe)_3 > P(OCH_2)_3CC_2H_5$, both of which are contrary to the observed order of reactivity.

On the other hand, both small cone angles and good Lewis acidity of the phosphine and phosphite ligands should promote an a mechanism. The reactivity is found to decrease in the order of increasing π-acidity of the ligands, but to vary non-systematically with cone angles. Thus, we suggest that SO_2 behaves as a nucleophile and exhibits associative activation in its reactions with **VI–X**.

X-ray structure of X

Figure 1 displays the geometry of **X**. No X-ray structure has been done for the parent molecule **I**. However, a related compound **I***, $\overline{Mn(CO)_4[C(=N\text{-}C_6H_4P\text{-}CH_3)C(=NC_6H_4P\text{-}CH_3)CH_2C_6H_4P\text{-}OCH_3]}$, with a methoxy group instead of a Cl substituting the phenyl ring has been investigated. Selected bond distances and angles for **X** and **I*** are given in Tables 3 and 4, respectively.

The gross geometries of **X** and **I*** are very similar. With the exception of the fact that an axial CO in **I*** has been replaced by $P(OCH_2)_3CC_2H_5$ in **X**, the immediate environments of Mn are practically superimposable. Distances and angles in the four-membered chelate ring are nearly identical. Along the axis, <P–Mn–C(1) in **X** is 172.4° as compared to the axial <C–Mn–C in **I*** of 171.3°.

The Mn–C bond lengths in **I*** follow the order expected on electronic structure considerations; the shortest bond is the one *trans* to the Mn–N bond (N is not a π-acceptor). The second shortest one is *trans* to the iminoacyl group which is at least a weak π-acceptor. The longest C–O bonds are the axial ones in which each carbonyl is *trans* to another CO (strong π-acceptor). (The axial CO bonds in **I*** do not differ statistically in length.) Since –C(=NR) is isoelectronic with –C=O, these distances may be compared with bond lengths for $Mn(CO)_5C(O)CH_3$ [24] of $Mn\text{–}CO_{trans} = 1.79$ Å and $Mn\text{–}CO_{cis} = 1.83$ Å. Mn–C bonds in complex **X** display a different pattern. The shortest one is Mn–C(2), again the one *trans* to the Mn–N bond. However, the next shortest is Mn–C(1) *trans* to the phosphite with Mn–C(3) (which is *trans* to the iminoacyl C) being the longest. The kinds of arguments advanced for **I*** would lead to the interpretation that the iminoacyl group is a better π-acceptor than $P(OCH_2)_3CCH_2CH_3$, which seems unreasonable. A better way of viewing the pattern in Mn–C distances in **X** is to note that substitution of CO by the worse π-acceptor $P(OCH_2)_3CCH_2CH_3$, increases the electron density on Mn which is expected to shorten all the Mn–C distances involving π-acceptors, but should have the largest effect on the carbonyl *trans* to phosphite. The metric parameters of a pair of simpler molecules

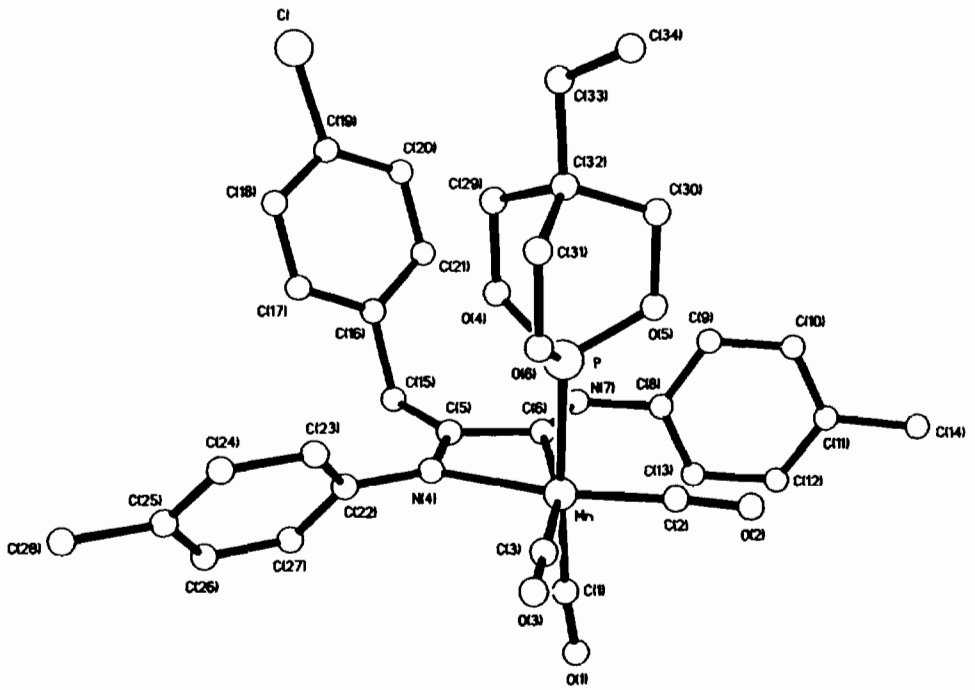

Fig. 1. Molecular structure of $(CO)_3\overline{Mn[C(=NC_6H_4P\text{-}CH_3)C(=N}C_6H_4P\text{-}CH_3)CH_2C_6H_4P\text{-}Cl][P(OCH_2)_3CCH_2CH_3]$ (**X**).

TABLE 3. Selected bond distances (Å)

Bond	X	I*
Mn–P	2.220(2)	1.851(5)[M–C(5)]
Mn–C(1)	1.813(5)	1.841(5)
Mn–C(2)	1.788(6)	1.805(5)
Mn–C(3)	1.840(6)	1.832(5)
Mn–N(4)	2.095(4)	2.079(3)
Mn–C(6)	2.044(5)	2.067(4)
C(1)–O(1)	1.151(6)	1.139(4)
C(2)–O(2)	1.149(7)	1.147(5)
C(3)–O(3)	1.132(7)	1.148(5)
N(4)–C(5)	1.290(7)	1.287(5)
C(5)–C(6)	1.487(8)	1.490(5)
C(6)–C(7)	1.281(7)	1.274(4)

TABLE 4. Selected bond angles (°)

Angle	X	I*
P–Mn–C(1)	172.4(2)	171.3(2)[C(1)–M–C(5)]
P–Mn–C(2)	90.1(2)	89.8(2)
P–Mn–C(3)	92.5(2)	94.4(2)
P–Mn–N(4)	89.0(1)	88.5(1)
P–Mn–C(6)	85.8(1)	84.8(2)
C(1)–Mn–C(2)	86.8(2)	91.1(2)
C(1)–Mn–C(3)	94.5(5)	94.2(2)
C(1)–Mn–N(4)	92.3(2)	88.9(1)
C(1)–Mn–C(6)	88.1(2)	86.6(2)
C(2)–Mn–C(3)	94.0(2)	92.8(2)
C(2)–Mn–N(4)	165.9(2)	167.9(2)
C(2)–Mn–C(6)	101.7(2)	103.6(2)
C(3)–Mn–N(4)	100.1(2)	99.3(2)
C(3)–Mn–C(6)	164.2(2)	163.6(2)
N(4)–Mn–C(6)	64.1(2)	64.4(1)
Mn–P–O(4)	115.4(2)	
Mn–P–O(5)	117.5(2)	
Mn–P–O(6)	117.2(2)	
Mn–C(1)–O(1)	174.1(5)	177.7(4)
Mn–C(2)–O(2)	176.9(4)	178.5(4)
Mn–C(3)–O(3)	179.1(5)	179.8(2)
N(4)–C(5)–C(6)	104.4(4)	105.1(3)
C(5)–C(6)–N(7)	120.3(5)	119.3(2)
C(6)–N(7)–C(8)	117.9(5)	121.3(3)
C(5)–C(15)–C(16)	113.7(4)	108.9(3)

bear out this expectation. Some comparable bond lengths for $Cr(CO)_6$ are Cr–C = 1.915(1) Å [25] and for $Cr(CO)_5[P(OPh)_3]$ are [26]: $Cr\text{–}C_{trans} = 1.861(4)$ and $Cr\text{–}C_{cis,av} = 1.896(4)$ Å. The bond from the σ-donor-only imino N in **X** would be expected to be weakened and lengthened. This is the trend which is indeed observed; the shortening of the Mn–CO bond *trans* to phosphite is apparently great enough to outweight the effect of π-acceptance by the iminoacyl. The effect on the Mn–C bond lengths for COs *cis* to phosphite is apparently very small to negligible.

On the other hand, complexes have been described that have different bond lengths where equivalent bonds were expected. For example in *fac*-$MnBr(CO)_3(CNMe)_2$ [27], $Mn\text{–}CO_{trans\,Br} = 1.789(11)$ Å, $Mn\text{–}(CO)_{cis\,Br} =$ 1.854(12) and 1.815(11) Å. The differences in the

distances given in Table 3 are only *c.* 0.05 Å and therefore may not be significant.

The bulky *p*-chlorophenyl group is on the same side of the equatorial plane as the phosphite ligand. The reason for this is not immediately obvious, since there should be free rotation around the C(5)–C(15) single bond. The phosphite is tilted slightly towards the chlorobenzyl group as seen from the values of the Mn–P–O angles. The *p*-chlorophenyl group moves away from the phosphite; <C(5)–C(15)–C(16), is 125.6°, larger than the comparable angle of 113.7° in **I***. The longer Mn–P (2.22 Å compared to 1.85 Å for Mn–axial CO in **I***) helps to avoid steric crowding by positioning the cage at a height above Mn such that the plane of the phenyl ring is bent back reasonably far due to the angle at the benzylic C.

The orientation of the phosphite with respect to the equatorial plane is shown in Fig. 2. Two other related pseudooctahedral molecules have been previously described. In $Co(dmg)_2(i\text{-}Pr)[P(OCH_2)_3CCH_3]$ [28], the cage phosphite is oriented with two P–O bonds (<O–P–O = 102.0°) encompassing the Co–N bonds of one of the Co(dmg) chelate rings (<N–Co–N = 99.0°). The third P–O bond is situated on a crystallographic mirror plane and bisects the Co–N bonds of the second Co(dmg) ring. In $Fe(CO)_2[o\text{-}(Me_2As)_2C_6H_4]$-$[C(O)CH_3][P(OCH_2)_3CCH_2CH_3]$ [29], the small bite angle (<As_1–Fe–As_2 = 85.8°) should again allow the conformation having one two P–O bond encompassing the five-membered chelate ring and the third in a bisecting position between the carbonyls. Instead, the smaller As–Fe–As angle is bisected by one of the P–O bonds, and the remaining two P–O bonds encompass and nearly eclipse the Fe–CO groups. The observed orientation of the cage phosphite in **X** is similar to that in the latter complex. The alternative staggered conformation is not observed, presumably due to close contacts between the iminoacyl phenyl *ortho*-hydrogens and the phosphite oxygens in that orientation.

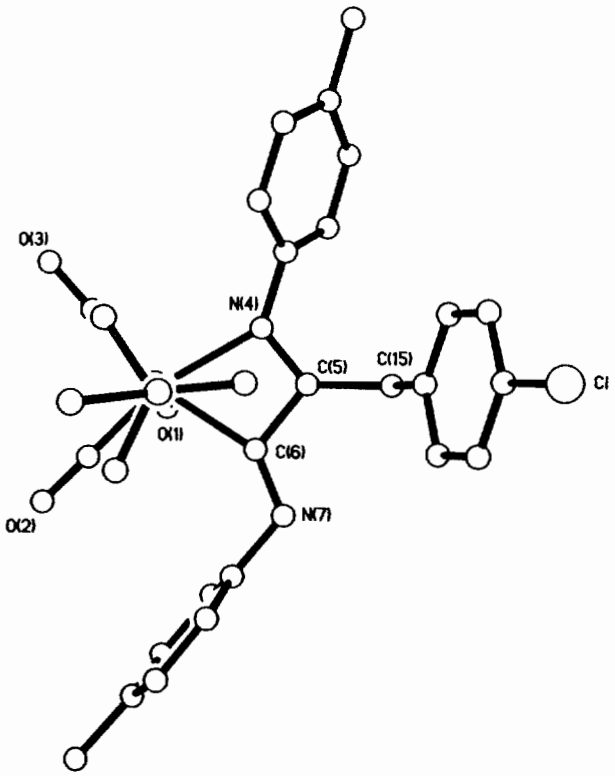

Fig. 2. Orientation of the cage phosphite with respect to the equatorial plane of **X**.

Supplementary material

Copies of the structure factors for the X-ray determination of the structure of **X** are available from the authors.

References

1 P. L. Motz, J. J. Alexander and D. M. Ho, *Organometallics, 8* (1989) 2589.
2 Z. Bouligarakis, *M.S. Thesis*, University of Cincinnati, OH, 1988.
3 A. J. Gordon, R. A. Ford, *The Chemist's Companion*, Wiley–Interscience, New York, 1972.
4 I. Ugi, R. Meyr, M. Lipinski, F. Bodesheim and F. Rosendahl, *Org. Synth., Coll. Vol. V* (1973) 300.
5 P. Hoffman, G. Gokel, D. Marquarding and I. Ugi, *Isonitrile Chemistry*, Academic Press, New York, 1971, p. 13.
6 I. Ugi, U. Fetzer, U. Ebholzer, H. Knupfer and K. Offerman, *Angew. Chem., Int. Ed. Engl., 4* (1965) 472.
7 P. J. Pollick, J. P. Bibler and A. Wojcicki, *J. Organomet. Chem., 16* (1969) 201.
8 T.-Y. Luh, *Coord. Chem. Rev., 60* (1984) 255.
9 P. L. Motz, *Ph.D. Dissertation*, University of Cincinnati, 1988.
10 M. M. Rahman, H.-Y. Liu, K. Eriks, A. Prock and W. P Giering, *Organometallics, 8* (1989) 1.
11 M. M. Rahman, H.-Y. Liu, A. Prock and W. P. Giering, *Organometallics, 6* (1987) 650.
12 J. A. S. Howell and P. M. Burkinshaw, *Chem. Rev., 83* (1983) 557.
13 D. J. Robinson, E. A. Darling and N. J. Coville, *J. Organomet. Chem., 310* (1986) 203, and refs. therein.
14 P. K. Maples and C. S. Kraihanzel, *J. Am. Chem. Soc., 90* (1968) 6645.
15 C. Barbeau and R. J. Dubey, *Can. J. Chem., 51* (1973) 3684.
16 L. Vaska and S. S. Bath, *J. Am. Chem. Soc., 88* (1966) 1333.
17 F. A. Cotton and G. Wilkinson, *Advanced Inorganic Chemistry*, Wiley-Interscience, New York, 5th edn., 1988, p. 515.
18 Y. Yamamoto and H. Yamazaki, *Inorg. Chem., 13* (1974) 2145.
19 Y. Yamamoto and H. Yamazaki, *Bull.Chem. Soc. Jpn., 48* (1975) 3691.
20 G. J. Kubas, *Inorg. Chem., 18* (1979) 182.

21 R. R. Ryan, G. J. Kubas, D. C. Moody and P. G. Eller, *Struct. Bonding (Berling), 46* (1981) 47.
22 M. Graziani and A. Wojcicki, *Inorg. Chim. Acta, 4* (1970) 347.
23 G. A. Gott, J. Fawcett, C. A. McAuliffe and D. R. Russell, *J. Chem. Soc., Chem. Commun.*, (1984) 1283.
24 T. Block, R. F. Fenske and C. P. Casey, *J. Am. Chem. Soc., 98* (1976) 441.
25 S. W. Kirtley, in G. Wilkinson, F. G. A. Stone and E. W. Abel (eds.), *Comprehensive Organometallic Chemistry,* Vol. 3, Pergamon, New York, 1982, p. 789.
26 H. J. Plastas, J. M. Stewart and S. O. Grim, *J. Am. Chem. Soc., 98* (1969) 4326.
27 P. M. Treichel, in G. Wilkinson, F. G. A. Stone and E. W. Abel (eds.), *Comprehensive Organometallic Chemistry,* Vol. 4, Pergamon, New York, 1982, p. 142.
28 M.Bresciani-Pahor, G. Nardin, L. Randaccio and E. Zagrando, *Inorg. Chim. Acta, 65* (1982) L143.
29 M. J. Newlands and M.F. Mackay, *Acta Crystallogr., Sect. C, 42* (1986) 677.